Journal of Solid State Chemistry 279 (2019) 120979

Contents lists available at ScienceDirect

Journal of Solid State Chemistry

journal homepage: www.elsevier.com/locate/jssc

Insight into volatile iodine uptake properties of covalent organic frameworks with different conjugated structures

Yuling Yang, Xiaohong Xiong, Yaling Fan, Zhenqin Lai, Zhenzhen Xu, Feng Luo *

State Key Laboratory of Nuclear Resources and Environment, School of Chemistry, Biology and Materials Science, East China University of Technology, Nanchang, 330013, PR China

ARTICLE INFO

Keywords:
COFs
Iodine vapor uptake
Conjugated structure
Charge-transfer interaction

ABSTRACT

The effective capture and storage of volatile radionuclide iodine from the nuclear waste stream is of great significance for environment remediation. Here we synthetize two types of two-dimensional (2D) covalent organic frameworks (COFs) for iodine vapor uptake, including COF-LZU1 with a whole π-π conjugated structure and TpPa-1 with a combination of π-π and p-π conjugated structure. The capacities for iodine vapor uptake are acquired for COF-LZU1 (530 wt%) and TpPa-1 (245 wt%). Thorough studies reveal that the large and intact π-π conjugated system formed by phenyl rings and imine (−C═N−) linkers in COF-LZU1 provides materials with ultrahigh iodine vapor uptake by inducing the charge-transfer interactions to transform adsorbed iodine molecules into polyiodide anions. However, the combined π-conjugated structure in TpPa-1 shows no obvious effect on iodine adsorption enhancement. Hence, this study can provide a guidance for the design and construction of ultrahigh-capacity iodine adsorbents.

1. Introduction

With the rapidly growing needs of current worldwide energy and the increasingly serious global warming, nuclear energy is becoming one of the most prominent and feasible alternative sources to minimize greenhouse gas emissions [1,2]. However, an urgent issue along with nuclear energy is the nuclear waste pollution, especially volatile radionuclide fission products [3–7]. Radioiodine is a typical radioactive emission that accompanies nuclear fission and attracts public concerns due to its long half-lives (1.57×10^7 years for ^{129}I and 8 days for ^{131}I), high volatility, and adverse effects on human metabolic processes and environment [8,9]. Therefore, it is urgent to find effective means to capture and store volatile radionuclide iodine for public and nuclear safety.

To date, physical adsorption has been regarded as the primary choice to remove iodine contaminants because of its general applicability, inexpensive cost, and simple operation procedures. Various porous materials, including inorganic porous materials [10], metal-organic frameworks (MOFs) [11,12], porous organic polymers (POPs) [13,14] and covalent organic frameworks (COFs) [15–18] have been exploited as iodine capturing materials. Among them, COFs distinguish themselves from the others by their periodically ordered structures and excellent physicochemical stabilities, which have been studied as promising materials for practical applications in gas storage [19,20], separation [21,22], catalysis [23,24], detection [25–27], optoelectronics [28], and energy storage materials [29,30]. Recent studies demonstrated that 2D COFs with 1D open channels could possess higher iodine uptake capacity than 3D COFs by realizing the full access between channels and iodine molecules [18]. In addition, the adsorption capacity of adsorbent for iodine is related to not only the accessible surface area, but also the nature and the effective adsorption units in the structure. The extended π-conjugations densely integrated in the networks are regarded as effective ways to enhance the affinity of the porous solid adsorbents towards iodine [31,32]. However, the iodine adsorption mechanisms of different conjugated structures in COFs have not been examined yet.

Herein, we set out to choose and prepare two types of 2D COFs with different conjugated structures, aiming at highly efficient removal of iodine. The selected COFs of TpPa-1 and COF-LZU1 were synthesized from *p*-phenylenediamine (PDA) as edge and 1,3,5-triformylphloroglucinol (TFP) or 1,3,5-benzenetricarboxaldehyde (TFB) as vertices, respectively (Scheme 1). It provided COF-LZU1 with a whole π-π conjugated structure and TpPa-1 with a combination of π-π and p-π conjugated structure. As expected, the obtained COFs exhibit satisfactory stability, high iodine uptake and recyclability. Surprisingly, compared with the TpPa-1, the COF-LZU1 with a whole π-π conjugated structure exhibits

* Corresponding author.
E-mail address: ecitluofeng@163.com (F. Luo).

https://doi.org/10.1016/j.jssc.2019.120979
Received 6 August 2019; Received in revised form 17 September 2019; Accepted 23 September 2019
Available online 25 September 2019
0022-4596/© 2019 Elsevier Inc. All rights reserved.

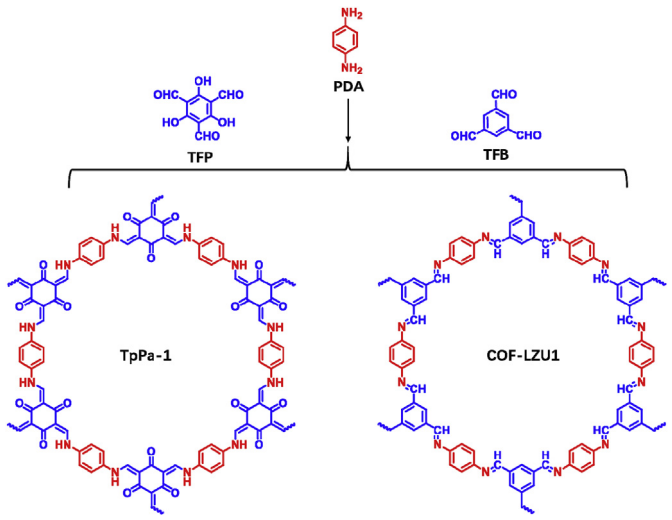

Scheme 1. Schematic description of the synthesis of TpPa-1 and COF-LZU1.

ultrahigh capacities (up to 530 wt %) for iodine enrichment, which gives the materials great possibility to be applied in the enrichment of radioactive iodine in nuclear waste disposal.

2. Experimental

2.1. Materials and instrumentation

The reagents and solvents are commercially available and used without further purification. Power X-ray diffraction (PXRD) patterns of samples were obtained at room temperature by a Bruker D8 ADVANCE X-ray at 40 mA and 40 kV using Cu Kα ($\lambda = 1.5405$ Å) radiations form 2°–30° (2θ angle range). Structure modeling and theoretical PXRD pattern calculating were carried out by Materials Studio software package. The N_2 adsorption-desorption isotherms were obtained at 77 K on a Belsorp-max adsorption apparatus using ultrahigh-purity-grade (>99.999%) N_2. Each sample was degassed at 110 °C for 12 h under ultrahigh vacuum before measurement. Fourier transform infrared spectroscopy (FT-IR) was performed in Thermo Scientific Nicolet iS5 FT-IR spectrometer with the 500–4000 cm^{-1}. Thermal gravimetric analysis (TGA) was performed by SDT Q600 TGA instrument from 30 to 800 °C in N_2 atmosphere at a constant rate of 10 °C/min. ^{13}C cross-polarization magic angle spinning (CP-MAS) NMR spectra for solid samples were taken at Bruker AVANCE III 400 MHz spectrometer, operating at a C-13 frequency of 400 MHz, using a contact time of 2 ms; samples were spun at 15.0 kHz. X-ray photoelectron spectra (XPS) was measured on a Thermo ESCALAB 250 spectrometer. Raman spectra was obtained by a RENISHAW RM2000 laser Raman Spectrometer. The morphology of COF samples was observed by Transmission electron microscopy (TEM, Hitachi HT9500, Japan). UV–vis adsorption spectrum was collected on a PerkinElmer Lambda 35 spectrophotometer at room temperature.

2.2. Synthesis of TFP

Hexamethylenetetraamine (15.098 g, 108 mmol) and phloroglucinol (6.014 g, 49 mmol) was added into 90 mL trifluoroacetic acid under N_2. The solution was heated at 100 °C for 2.5 h. Then 150 mL of 3 M HCl was added and the solution was heated at 100 °C for 1 h. After cooling to room temperature, the solution was filtered through Celite, extracted with 350 mL dichloromethane, dried over magnesium sulfate, and filtered. Rotary evaporation of the solution afforded 1.23 g (5.87 mmol, 11%) of an off-white powder. The pure sample was obtained by sublimation. ^1H NMR (400 MHz, $CDCl_3$) data indicated near 99% purity, giving 14.12 (s, 3H, OH), 10.15 (s, 3H, CHO) ppm. Element analysis: calculated value C, 51.44; H, 2.88; N, 0.00; Found: C 51.38; H 2.80; N, 0.00.

2.3. Synthesis of TpPa-1

0.3 mmol (63 mg) of TFP and 0.45 mmol (48.6 mg) PDA were added into a Pyrex tube with 1.5 mL butyl alcohol and 1.5 mL 1,2-dichlorobenzene. The mixture was sonicated for 20 min, followed by addition of 0.5 mL of 3 M aqueous acetic acid. After that, the tube was degassed by freeze-pump-thaw cycles for three times, sealed under vacuum and heated at 120 °C for 3 days. The reaction mixture was cooled to room temperature and washed with anhydrous tetrahydrofuran, anhydrous acetone, and anhydrous dichloromethane. The resulting dark red powder was dried at 120 °C under vacuum for 12 h.

2.4. Synthesis of COF-LZU1

0.1 mmol (16 mg) of TFB and 0.15 mmol (16 mg) PDA were added into a Pyrex tube with 2.0 mL butyl alcohol and 2.0 mL *o*-dichlorobenzene. The mixture was sonicated for 5 min, followed by addition of 0.5 mL of 6 M aqueous acetic acid. After that, the tube was degassed by freeze-pump-thaw cycles for three times, sealed under vacuum and heated at 120 °C for 3 days. The reaction mixture was cooled to room temperature and washed with anhydrous tetrahydrofuran, anhydrous acetone, and anhydrous dichloromethane. The resulting yellow powder was dried at 120 °C under vacuum for 12 h.

2.5. Uptake of iodine

The COF samples were activated by solvent exchange with anhydrous methanol for 3 times and calcined at 110 °C for 5 h under nitrogen atmosphere to ensure the water molecules inside removed. Then, an open small vial (2 mL) containing the COF sample (10.0 mg) was placed in a large vial (10 mL) containing iodine (2 g). The large vial was sealed and kept in an oven at 77 °C. After a certain period, the small vial containing the COF sample was weighted and placed back into the iodine-containing large vial. The large vial was sealed and put back in the oven at 77 °C to continue the adsorption till the mass of the small vial containing the COF sample did not change.

2.6. Release of iodine

The samples with iodine uptake (3 mg) were immersed in the methanol (30 mL) and kept for a certain time. Then the absorbency of supernatant was measured by using UV–vis spectrophotometer at various time intervals.

2.7. Recycling of the COF samples

The iodine-captured COF sample was added to methanol (30 mL) in a vial at 25 °C, and methanol was refreshed every 2 h until no color of the solution was observed. The COF sample was collected by filtration, washed with methanol, dried under vacuum at 120 °C overnight and reused for the next cycle.

3. Results and discussion

3.1. Material synthesis and characterization

The synthesis of the TpPa-1 and COF-LZU1 were accomplished *via* Schiff-base chemistry by using solvothermal reactions carried out in a sealed Pyrex tube for 72 h at 120 °C. The as-prepared COF samples are insoluble in common organic solvents and water, and exhibit high thermal stability. As revealed by TGA, the TpPa-1 was thermally stable up to 330 °C under nitrogen atmosphere. And the synthesized COF-LZU1 was more stable until 450 °C (Fig. S1). However, the TpPa-1 showed ~10%

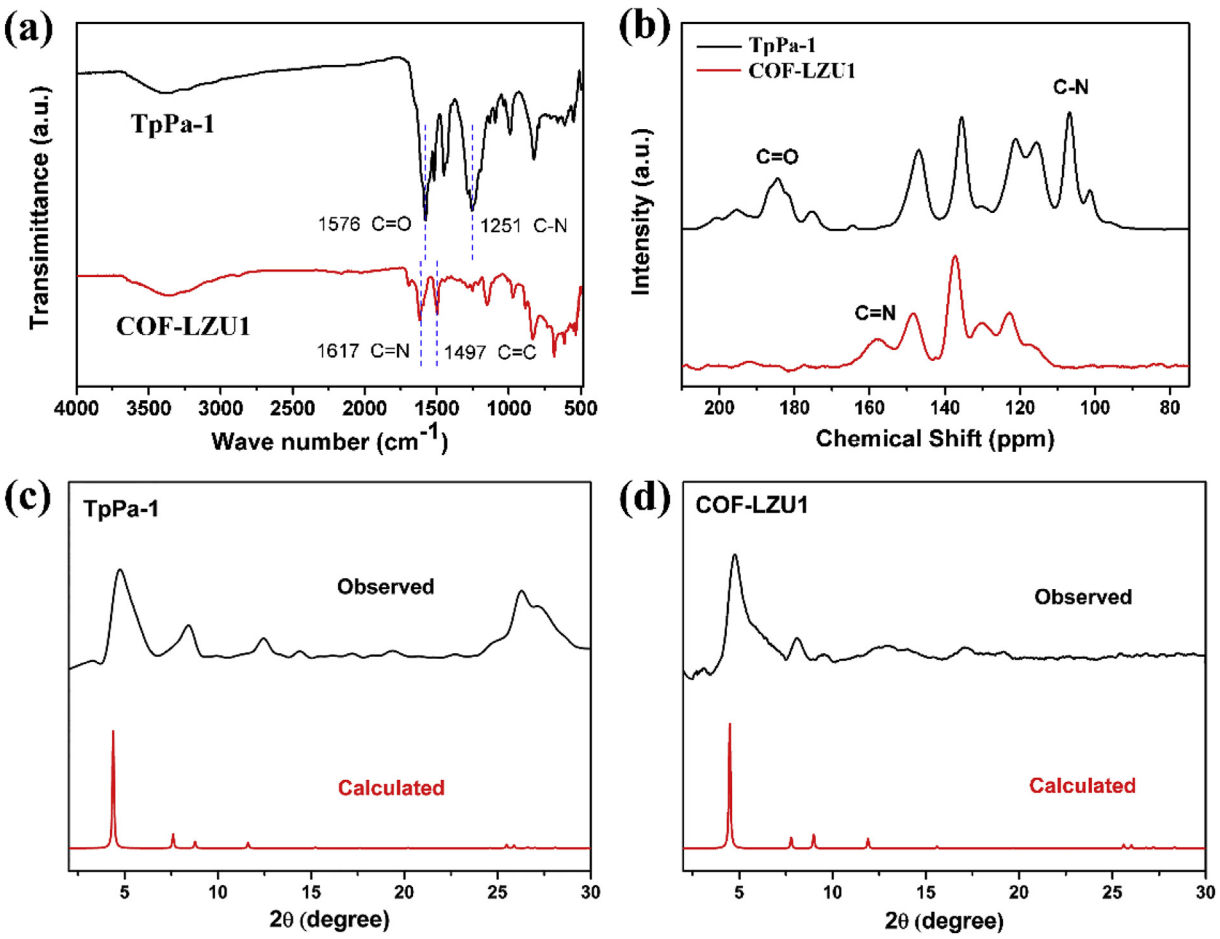

Fig. 1. (a) FT-IR spectra and (b) ^{13}C solid state NMR spectra of TpPa-1 and COF-LZU1; Observed (black) and calculated (red) PXRD patterns of TpPa-1 (c) and COF-LZU1 (d). (For interpretation of the references to color in this figure legend, the reader is referred to the Web version of this article.)

weight loss at the temperature of less than 100 °C, which indicated the TpPa-1 had a higher moisture adsorption capacity than the COF-LZU1. It resulted from the hydrophilic groups in the TpPa-1 structure, such as C═O and –NH–.

FT-IR was used to characterize the as-prepared COFs (Fig. 1a). In the spectra of TpPa-1, the characteristic C═O vibration band (1576 cm^{-1}) and C–N vibration band (1251 cm^{-1}) appeared, strongly suggested the formation of β-ketoenamine-based framework structures. A band assignable to the vibration of C═N was observed at 1617 cm^{-1} in the spectra of COF-LZU1, giving direct evidence for the formation of imine linkages. Additionally, the structures of COFs were further confirmed using solid state ^{13}C NMR spectroscopy. As shown in Fig. 1b, a characteristic resonance peak of imine carbons appeared approximately at 158 ppm in the spectra of the COF-LZU1, which demonstrated the presence of the imine linkages in materials again. The TpPa-1 showed the peak at 184 ppm assigned to the carbons of aldehyde (Fig. 1b).

Powder X-ray diffraction (PXRD) measurements confirmed the formation of crystalline frameworks. The TpPa-1 exhibited PXRD peaks at

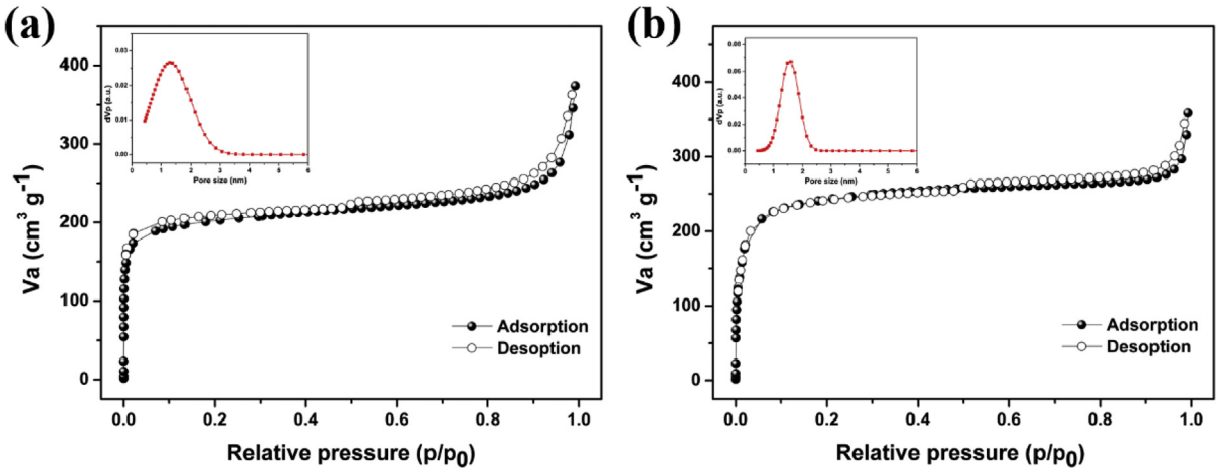

Fig. 2. N_2 adsorption-desorption isotherm curves and pore size distributions of TpPa-1 (a) and COF-LZU1 (b).

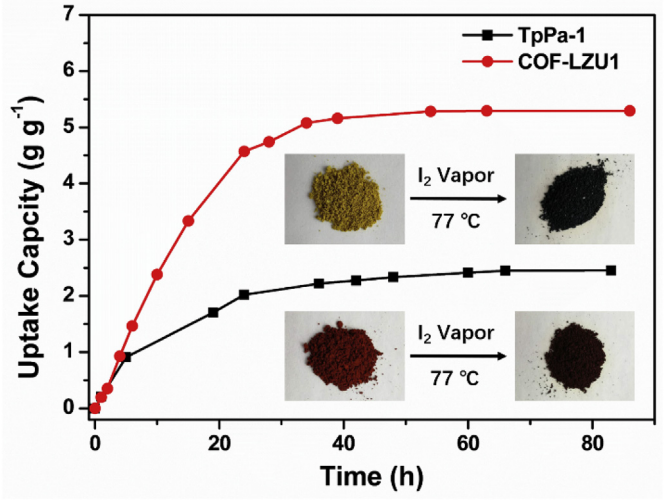

Fig. 3. Uptake of iodine of the COF-LZU1 and TpPa-1 as a function of exposure time at 77 °C and ambient pressure.

4.73°, 8.34°, 12.58° and 26.76°, which were assigned to the (100), (110), (210) and (001) facets, respectively. The PXRD pattern of COF-LZU1 had obvious diffraction peaks in 4.73° and 8.15°, which arose from (100) and (110) facets (Fig. 1c and d). Based on the hexagonal P6/m space group, the simulated structural models of TpPa-1 and COF-LZU1 were built by the Materials Studio software package. Then, their theoretical PXRD patterns were calculated by Reflex, a module implemented in Material Studio. The PXRD patterns of the as-synthesized TpPa-1 and COF-LZU1 matched well with their corresponding simulated patterns. The presence of slightly broad peaks in TpPa-1 observed at higher 2θ angles of the (001) facet may originate from the defects in the π-π stacking between the successive COF layers [33,34].

3.2. Porosity measurement

The pore features of COFs were probed *via* N_2 adsorption-desorption experiments at 77 K up to 1 bar. The N_2 adsorption curve of TpPa-1 and COF-LZU1 matched the classical type I sorption model characterized by a steep nitrogen uptake in the low-pressure range ($P/P_0 = 0–0.01$), which was indicative of permanent microporosity (Fig. 2) [35] The Brunauer-Emmett-Teller (BET) surface areas calculated from the adsorption branch of the N_2 isotherms were 765 for TpPa-1 and 858 $m^2 g^{-1}$ for COF-LZU1. According to the nonlocal density function theory method, the TpPa-1 and COF-LZU1 samples possessed 1.30 and 1.60 nm sized aperture and had pore volumes as high as 0.46 and 0.48 $cm^3 g^{-1}$, respectively. Comparing with the TpPa-1, the COF-LZU1 showed a narrower pore size distribution, which indicated it had a more ordered structure and higher crystallinity.

3.3. Iodine capture and release

Based on the above chemical stability and high porosity, we investigated iodine vapor capture by exposing the COF solid to iodine vapor at 77 °C under ambient pressure, which is close to the typical nuclear fuel reprocessing conditions. The performance for iodine capture was investigated by gravimetric method (Fig. 3). The COF-LZU1 exhibited a rapid

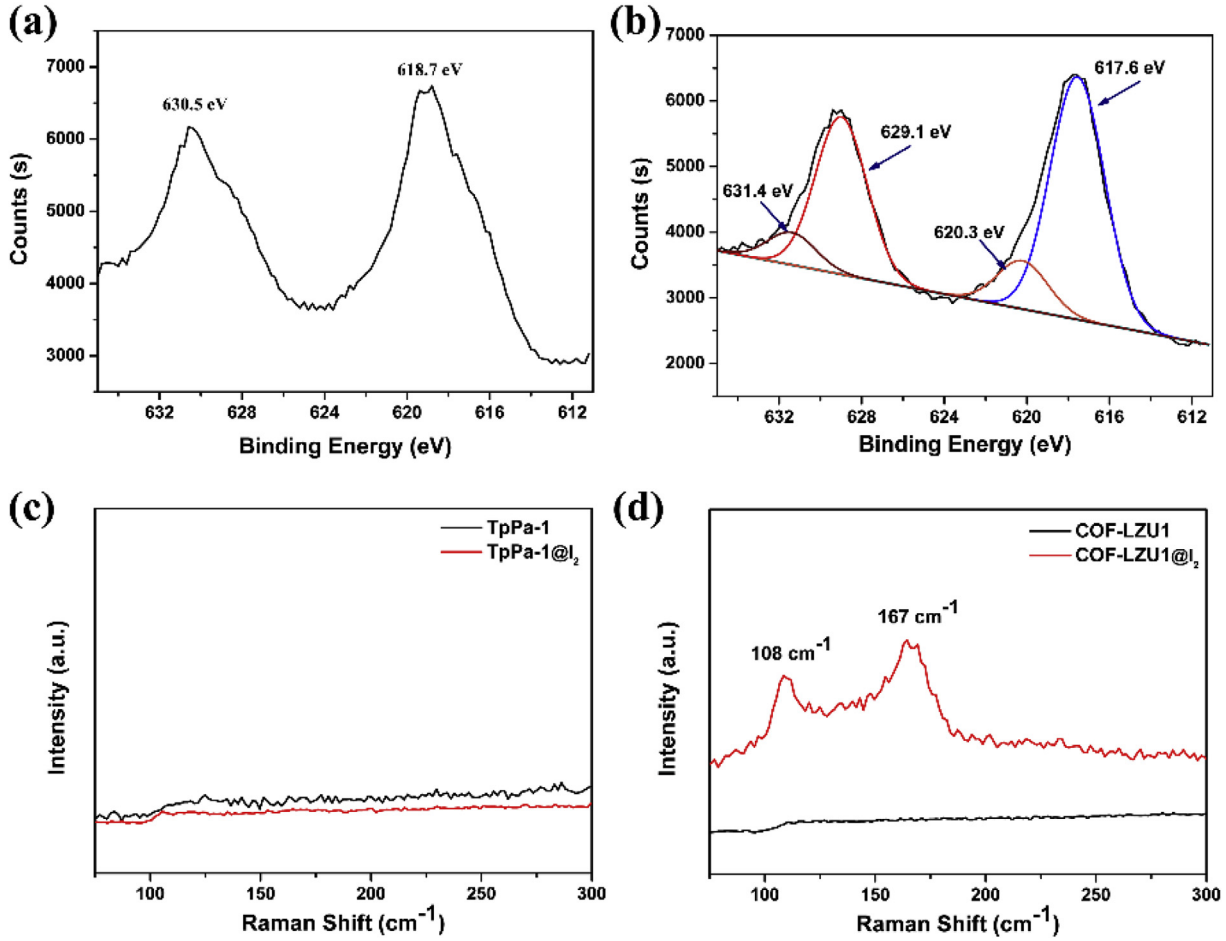

Fig. 4. XPS spectra of TpPa-1@I_2 (a) and COF-LZU1@I_2 (b). Raman spectra of TpPa-1 (c) and COF-LZU1 (d) before and after volatile iodine adsorption.

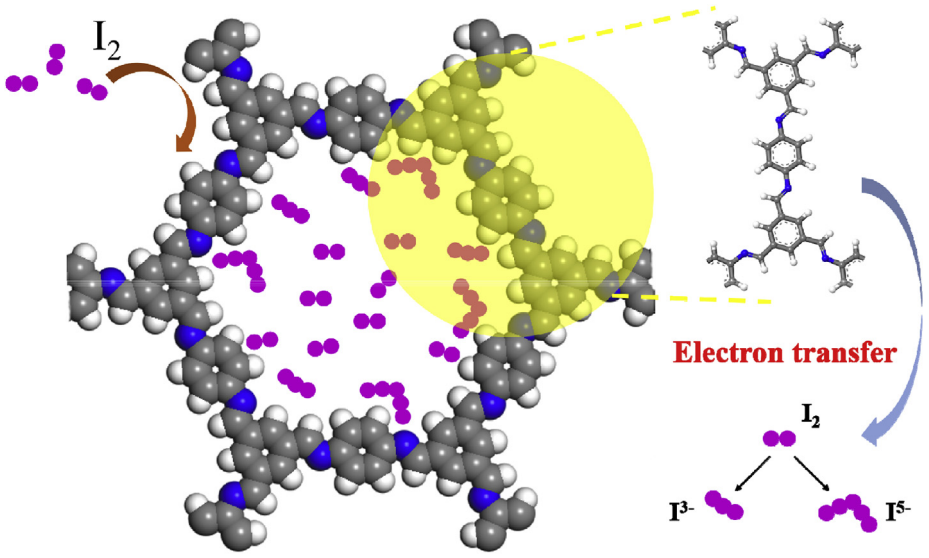

Scheme 2. Schematic illustration of the iodine uptake mechanism of COF-LZU1s[a].
a N, blue; C, gray; H, white.

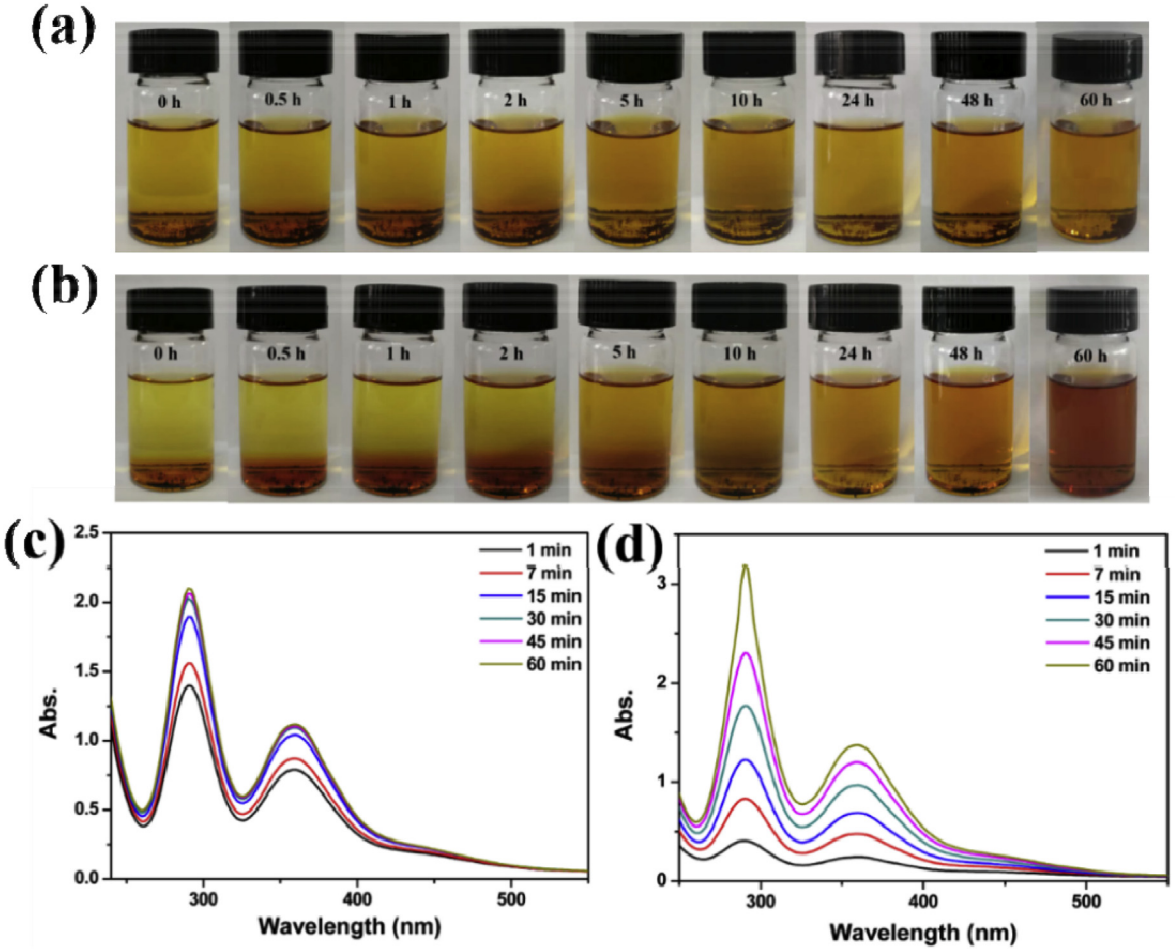

Fig. 5. Photographs for the iodine-released process of the I_2@ TpPa-1 (a) and I_2@ COF-LZU1 (b). UV–vis spectra for the iodine release from I_2@ TpPa-1 (c) and I_2@ COF-LZU1 (d) at different times.

adsorption, yielding a nearly linear increasement over 24 h and then saturating within 48 h. Similarly, the TpPa-1 exhibited quick iodine uptake and reached adsorption saturation in 48 h. Remarkably, the COF-LZU1 and the TpPa-1 achieved uptake capacities as high as 5.30 and 2.45 g g^{-1}, respectively.

Such ultrahigh value of the COF-LZU1 promoted us to investigate why it had such high iodine uptake capacity. Since TpPa-1 and COF-LZU1 showed a total pore volume of 0.46 and 0.48 $cm^3 g^{-1}$, a theoretical maximum iodine uptake of 2.26 g g^{-1} and 2.36 g g^{-1} would be calculated from the product of density of solid iodine and the total volume of the COF by assuming all the pores were filled with iodine molecules. This theoretical value of TpPa-1 was close to the experimental result. However, this value of COF-LZU1 was still far lower than the experimental result 5.30 g g^{-1}, not to mention in the case of the pores just being partially filled.

The mechanism of the iodine enrichment was preliminarily studied by FT-IR. It was found that the characteristic peak position of the materials changed significantly before and after the adsorption (Figs. S2 and S3). For example, the C═C and C–H bands of the phenyl ring in COF-LZU1 shifted from 1497, 834 and 682 cm^{-1} to 1492, 822 and 658 cm^{-1}. Moreover, the imine linkages changed markedly from 1617 to 1590 cm^{-1}. It indicated that the iodine adsorption could occur simultaneously at imine linkage and phenyl rings in the COF-LZU1. In the FT-IR spectra of TpPa-1, the C═O bands at 1576 shifted to 1560 cm^{-1} and the C–N bands at 1255 shifted to 1295 cm^{-1}. In addition, the C═C and C–H bands of the phenyl ring bands at 1451 and 824 shifted to 1474 and 810 cm^{-1} and the C═C bands of pentyl ring disappeared. It testified that the iodine adsorption occurred at enamine linkage, C═O band and phenyl ring in the materials. The TpPa-1 and COF-LZU1 before and after being exposed to iodine vapor were investigated by TEM (Fig. S4). Both of the two COFs displayed stability of their morphology after iodine adsorption. And the deeper contrast of TpPa-1@I_2 and COF-LZU1@I_2 after exposing to iodine vapor suggested that the inner cavities of the microspheres were filled with iodine. Additionally, EDX measurement showed that the molar ratio of C/N/O in TpPa-1 and the molar ratio of C/O in COF-LZU1 were approximate before and after iodine adsorption (Fig. S5), which also demonstrated the stability of their conjugated structure.

The existing form of iodine captured by COFs was further ascertained by XPS. As seen in Fig. 4a, the iodine spectrum of TpPa-1@I_2 displayed two split peaks located at 630.5 and 618.7 eV, which were assigned to the I $3d_{3/2}$ and I $3d_{5/2}$ orbitals of iodine molecules, respectively, indicating that the iodine captured form existed as molecule I_2. In the XPS spectra of COF-LZU1@I_2, the additional single peaks at binding energies of 631.4 and 620.3 eV were attributed to the formation of polyiodine anions (Fig. 4b) [36] In addition, the species of iodine in COF-LZU1@I_2 and TpPa-1@I_2 were detected by Raman spectroscopy (Fig. 4c and d). In the spectra of COF-LZU1@I_2, the low-frequency spectral region was dominated by the peaks at 108 and 167 cm^{-1}, which were assigned to the stretching vibrations of I^{3-} and I^{5-}, respectively [37,38]. However, the Raman spectra of TpPa-1 showed no change before and after iodine adsorption. The results indicated the adsorbed iodine species in TpPa-1 existed as I_2 and the process was physical adsorption driven by van der Waals forces, while the adsorption mode of COF-LZU1 was the combination of physical adsorption and chemisorption.

As previously reported, high-BET-surface-area, heteroatom-rich and electron-rich solids always deliver better performance in removing iodine vapor. In our study, the combination of p-π and π-π conjugated systems designed in the TpPa-1 showed a little effect on the enhancement of the iodine uptake capacity. However, the phenyl rings and imine linkers in COF-LZU1, which formed a whole π-π conjugated structure into the framework, had been demonstrated to provide abundant electron-rich sites to iodine guest molecules and led to the generation of polyiodine anions. Hence, the ultrahigh loading of iodine in the pores of COF-LZU1 was attributed to these charge-transfer interactions. The possible mechanism of volatile iodine uptake on COF-LZU1s was put forward and shown in Scheme 2. Therefore, design and construction of large and intact π-π conjugated structure could be an effective way for the most adsorbent materials that lack accessible interactions with iodine.

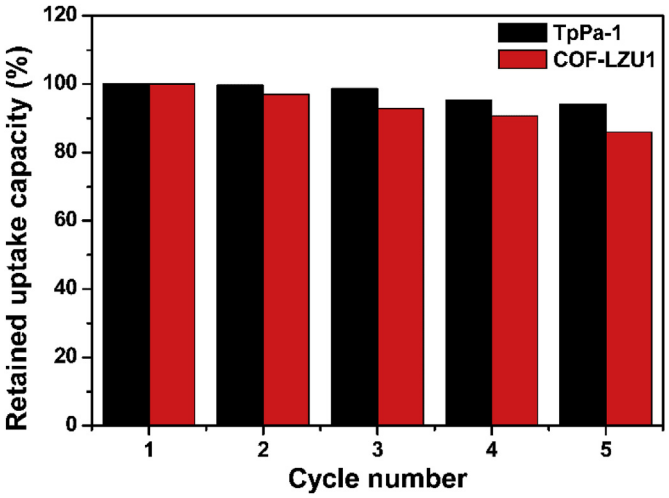

Fig. 6. Retained uptake capacity upon cycling the TpPa-1 and COF-LZU1 in iodine vapor capture.

Notably, the trapped iodine could be released by immersing in organic solvents. Once the iodine-loaded samples of TpPa-1 and COF-LZU1 were immersed in methanol at 25 °C, the color of the methanol gradually varied from colorless to dark brown (Fig. 5a and b), indicating that the iodine released gradually from the pore of materials. To further study such releasing process, the delivery of iodine was measured by UV–vis spectroscopy (Fig. 5c and d). The signals corresponding to iodine at 290 and 359 nm showed that the iodine released of TpPa-1@I_2 normally increased and reached a dynamic equilibrium within nearly 30 min. However, the COF-LZU1@I_2 showed a much slower release rate than TpPa-1@I_2, which illustrated that the COF-LZU1 had a stronger adsorption affinity for iodine molecules. This result further confirmed the chemisorption of volatile iodine in COF-LZU1, which was coincided with the assumptive mechanism obtained by XPS and Raman spectroscopy. This finding revealed that these materials could be attractive recyclable iodine uptake adsorbents in practical application. To prove this, the recyclability was further studied. The result showed that the TpPa-1 and COF-LZU1 could retain 94% and 86% of its initial capacity after five cycles, respectively (Fig. 6). These cycle performances suggested that the porous structures were robust against oxidative iodine upon long-period exposure at high temperature.

4. Conclusions

In summary, two 2D COFs with different conjugated structures have been synthesized and studied for iodine adsorption. Both of the two COFs showed satisfactory chemical stability, high iodine uptake capacity and good recyclability. Comparing with the TpPa-1, the COF-LZU1 exhibited an extremely higher iodine capture capacity up to 5.30 g g^{-1} and a longer iodine release time. Thorough studies indicated that constructing a large and intact π-π conjugated structure in the framework could significantly improve the iodine capture capacity by inducing the charge-transfer interactions between electron-rich sites and iodine molecules, while the mixed and discontinuous conjugated units showed little effect. These findings are of fundamental importance to understanding iodine vapor capture and designing materials to treat harmful volatile substances.

Acknowledgment

We thanks to the National Science Foundations of China (21871047, 21661001, the Natural Science Foundation of Jiangxi Province of China (20181ACB20003).

Appendix A. Supplementary data

Supplementary data to this article can be found online at https://doi.org/10.1016/j.jssc.2019.120979.

References

[1] J.D. Vienna, Int. J. Appl. Glass Sci. 1 (2010) 309–321.
[2] E. Kintisch, Science 310 (2005) 1406.
[3] K.C. Jie, Y.J. Zhou, E. Li, Z.T. Li, R. Zhao, F.H. Huang, J. Am. Chem. Soc. 139 (2017) 15320–15323.
[4] J.Q. Li, L.L. Gong, X.F. Feng, L. Zhang, H.Q. Wu, C.S. Yan, Y.Y. Xiong, H.Y. Gao, F. Luo, Chem. Eng. J. 316 (2017) 154–159.
[5] L. Zhang, L.L. Wang, L.L. Gong, X.F. Feng, M.B. Luo, F. Luo, J. Hazard Mater. 311 (2016) 30–36.
[6] L. Zhu, D.P. Sheng, C. Xu, X. Dai, M.A. Silver, J. Li, P. Li, Y.X. Wang, Y.L. Wang, L.H. Chen, C.L. Xiao, J. Chen, R.H. Zhou, C. Zhang, O.K. Farha, Z.F. Chai, T.E. Albrecht-Schmitt, S.A. Wang, J. Am. Chem. Soc. 139 (2017) 14873–14876.
[7] W. Yao, X.X. Wang, Y. Liang, S.J. Yun, P.C. Gu, Y.B. Sun, C. Xu, J. Chen, T. Hayat, A. Alsaedi, X.K. Wang, Chem. Eng. J. 332 (2018) 775–786.
[8] W.J. Weber, F.P. Roberts, Nucl. Technol. 60 (1983) 178–198.
[9] D.R. Haefner, T.J. Tranter, Idaho National Laboratory, 2007.
[10] K.W. Chapman, P.J. Chupas, T.M. Nenoff, J. Am. Chem. Soc. 132 (2010) 8897–8899.
[11] D. Banerjee, X. Chen, S.S. Lobanov, A.M. Plonka, X. Chan, J.A. Daly, T. Kim, P.K. Thallapally, J.B. Parise, ACS Appl. Mater. Interfaces 10 (2018) 10622–10626.
[12] X.R. Zhang, I.D. Silva, H.G.W. Godfrey, S.K. Callear, S.A. Sapchenko, Y.Q. Cheng, I. Vitórica-Yrezábal, M.D. Frogley, G. Cinque, C.C. Tang, C. Giacobbe, C. Dejoie, S. Rudić, A.J. Ramirez-Cuesta, M.A. Denecke, S.H. Yang, M. Schröder, J. Am. Chem. Soc. 139 (2017) 16289–16296.
[13] Y.Z. Liao, Z.H. Cheng, W.W. Zuo, A. Thomas, C.F.J. Faul, ACS Appl. Mater. Interfaces 9 (2017) 38390–38400.
[14] A. Sigen, Y.W. Zhang, Z.P. Li, H. Xia, M. Xue, X.M. Liu, Y. Mu, Chem. Commun. 50 (2014) 8495–8498.
[15] X. Guo, Y. Tian, M. Zhang, Y. Li, R. Wen, X. Li, X.F. Li, Y. Xue, L.J. Ma, C.Q. Xia, S.J. Li, Chem. Mater. 30 (2018) 2299–2308.
[16] C. Wang, Y. Wang, R. Ge, X.D. Song, X.Q. Xing, Q.K. Jiang, H. Lu, C. Hao, X.W. Guo, Y.N. Gao, D.L. Jiang, Chem. Eur J. 24 (2018) 585–589.
[17] Z.J. Yin, S.Q. Xu, T.G. Zhan, Q.Y. Qi, Z.Q. Wu, X. Zhao, Chem. Commun. 53 (2017) 7266–7269.
[18] P. Wang, Q. Xu, Z.P. Li, W.M. Jiang, Q.H. Jiang, D.L. Jiang, Adv. Mater. 30 (2018), 1801991.
[19] C.J. Doonan, C.J. Tranchemontagne, T.G. Glover, J.R. Hunt, O.M. Yaghi, Nat. Chem. 2 (2010) 235–238.
[20] Y.F. Zeng, R.Q. Zou, Y.L. Zhao, Adv. Mater. 28 (2016) 2855–2873.
[21] H. Oh, S.B. Kalidindi, Y. Um, S. Bureekaew, R. Schmid, R.A. Fischer, M. Hirscher, Angew. Chem. Int. Ed. 52 (2013) 13219–13222.
[22] L. Stegbauer, M.W. Hahn, A. Jentys, G. Savasci, C. Ochsenfeld, J.A. Lercher, B.V. Lotsch, Chem. Mater. 27 (2015) 7874–7881.
[23] Q.R. Fang, S. Gu, J. Zheng, Z.B. Zhuang, S.L. Qiu, Y.S. Yan, Angew. Chem. Int. Ed. 53 (2014) 2878–2882.
[24] L.Y. Li, L. Li, C.Y. Cui, H.J. Fan, R.H. Wang, ChemSusChem 10 (2017) 4921–4926.
[25] S.-Y. Ding, M. Dong, Y.-W. Wang, Y.-T. Chen, H.-Z. Wang, C.-Y. Su, W. Wang, J. Am. Chem. Soc. 138 (2016) 3031–3037.
[26] C.L. Zhang, S.M. Zhang, Y.H. Yan, F. Xia, A. Huang, Y.Z. Xia, ACS Appl. Mater. Interfaces 15 (2017) 13415–13421.
[27] Y.W. Peng, Y. Huang, Y.H. Zhu, B. Chen, L.Y. Wang, Z.C. Lai, Z.C. Zhang, M.T. Zhao, C.L. Tan, N.L. Yang, F.W. Shao, Y. Han, H. Zhang, J. Am. Chem. Soc. 139 (2017) 8698–8704.
[28] B. Sun, C.H. Zhu, Y. Liu, C. Wang, L.J. Wan, D. Wang, Chem. Mater. 29 (2017) 4367–4374.
[29] S. Chandra, D. Roy Chowdhury, M. Addicoat, T. Heine, A. Paul, R. Banerjee, Chem. Mater. 29 (2017) 2074–2080.
[30] J.H. Sun, A. Klechikov, C. Moise, M. Prodana, M. Enachescu, A.V. Talyzin, Angew. Chem. Int. Ed. 57 (2018) 1034–1038.
[31] Z.J. Yan, Y. Yuan, Y.Y. Tian, D.M. Zhang, G.S. Zhu, Angew. Chem. Int. Ed. 54 (2015) 12733–12737.
[32] X. Qian, Z.Q. Zhu, H.X. Sun, F. Ren, P. Mu, W. Liang, L. Chen, A. Li, ACS Appl. Mater. Interfaces 8 (2016) 21063–21069.
[33] G. Das, D.B. Shinde, S. Kandambeth, B.P. Biswal, R. Banerjee, Chem. Commun. 50 (2014) 12615–12618.
[34] S. Kandambeth, A. Mallick, B. Lukose, M.V. Mane, T. Heine, R. Banerjee, J. Am. Chem. Soc. 134 (2012) 19524–19527.
[35] K.S.W. Sing, D.H. Everett, R.A.W. Haul, L. Moscou, R.A. Pierotti, J. Rouquérol, T. Siemieniewska, IUPAC. Pure Appl. Chem. 57 (1985) 603.
[36] S.L. Hsu, A.J. Signorelli, G.P. Pez, R.H. Baughman, J. Chem. Phys. 69 (1978) 106–111.
[37] D.K.L. Harijan, V. Chandra, T. Yoon, K.S. Kim, J. Hazard Mater. 344 (2018) 576–584.
[38] Y. Zhu, Y.J. Ji, D.G. Wang, Y. Zhang, H. Tang, X.R. Jia, M. Song, G. Yu, G.C. Kuang, J. Mater. Chem. A 5 (2017) 6622–6629.